Measurement 270 (2026) 120907

Contents lists available at ScienceDirect

Measurement

journal homepage: www.elsevier.com/locate/measurement

Multiphysics measurements of in-service asphalt pavements for the analysis of their long-term aging behaviors: systems, methods, and key insights

Xingyu Chen [a], Yuhong Wang [a,*], Yinghao Miao [b], Xingyi Zhu [c], Haopeng Wang [d], Huailei Cheng [c]

[a] Department of Civil and Environmental Engineering, The Hong Kong Polytechnic University, Hung Hom, Kowloon, Hong Kong
[b] National Center for Materials Service Safety (NCMS), University of Science and Technology Beijing (USTB), Beijing, China
[c] The Key Laboratory of Road and Traffic Engineering of Ministry of Education, Tongji University, Shanghai 201804, China
[d] Department of Civil and Environmental Engineering, The University of Liverpool, UK

ARTICLE INFO

Keywords:
Asphalt pavements
Field measurements and monitoring
Oxygen distribution
Moisture distribution
Multiphysics aging model

ABSTRACT

The long-term aging of in-service asphalt pavements is affected by coupled Multiphysics factors, including temperature, oxygen exposure, and moisture content. Although pavement temperature is routinely monitored, in-situ measurement of oxygen and moisture within asphalt pavements remains largely unexplored, resulting in limited accuracy in aging analysis and prediction. To address such a critical gap, this study developed an integrated system for the simultaneous measurement and monitoring of temperature, oxygen, and moisture within asphalt pavements, enabling the characterization of their spatiotemporal variations. In laboratory investigation, the system was employed to investigate oxygen distribution characteristics for different asphalt mixture types. In field investigation, the system was deployed in a full-scale test section for year-long monitoring, providing first-hand information on in-situ oxygen and moisture distributions within asphalt pavements. The lab test demonstrated that oxygen distribution in asphalt mixtures is predominantly governed by the rate of oxygen transport, which is strongly influenced by the characteristics of air voids. The field investigation revealed a distinct arc-shaped distribution profile of oxygen content with pavement depth, challenging the traditional assumption of monotonic variation of oxygen distribution in pavements. A bidirectional oxygen diffusion model was proposed to capture this finding. Additionally, moisture was found to play a substantial role in modulating the distributions of both oxygen and temperature. Overall, these findings enhance the understanding of asphalt aging mechanisms in pavements and establish a foundation for more accurate aging predictions and the development of targeted anti-aging strategies.

1. Introduction

As a critical transport infrastructure, asphalt pavements account for over 90% of the global road network due to their superior driving comfort and cost effectiveness [1]. Despite this advantage, asphalt pavements are susceptible to oxidative aging, which significantly affects the physicochemical properties of asphalt binders [2–6], leading to embrittlement, cracking, and eventual structural failure [7–10]. Therefore, a comprehensive understanding of asphalt pavement aging mechanism is essential for pavement design and maintenance planning, thereby enhancing the durability and resilience of road infrastructure.

The oxidative aging of asphalt pavements is influenced by multiple factors, including the intrinsic properties of asphalt binders, the volumetric properties of asphalt mixtures, pavement structural designs, and environmental factors. Previous studies have primarily focused on the binder-level oxidation kinetics [11–15] and the influence of asphalt mixture's volumetric properties on binder aging [16–20]. However, the aging behavior of asphalt binders under actual pavement service conditions is relatively less researched. In particular, the spatiotemporal variations of environmental factors (e.g., temperature, oxygen, and moisture) within pavement structures and their impact on asphalt aging are seldom explored, leading to inaccurate prediction of asphalt aging in in-service pavements and insufficient aging-control methods.

According to the oxidation kinetics of asphalt binder, temperature

* Corresponding author.
E-mail addresses: xingyu666.chen@connect.polyu.hk (X. Chen), yuhong.wang@polyu.edu.hk (Y. Wang), miaoyinghao@ustb.edu.cn (Y. Miao), zhuxingyi66@tongji.edu.cn (X. Zhu), Haopeng.Wang@liverpool.ac.uk (H. Wang), chl6218@tongji.edu.cn (H. Cheng).

https://doi.org/10.1016/j.measurement.2026.120907
Received 21 November 2025; Received in revised form 11 January 2026; Accepted 19 February 2026
Available online 20 February 2026

and oxygen are two environmental factors that directly govern its oxidation rate [11–15]. Extensive field data [21–23] have well documented temperature distribution patterns within pavements. In contrast, field studies on the distribution of oxygen, the essential reactant for binder aging, are nearly non-existent. As a result, existing pavement aging models (e.g., the global aging system [24]) simply assume that oxygen content inside pavement remains constant at the atmospheric level or monotonically decreases with pavement depth, yielding an exponentially decaying aging profiles in asphalt pavements [24–26]. However, by analyzing field-extracted cores, some recent studies [27–31] demonstrated that aging does not necessarily decrease with pavement depth. As illustrated in Fig. 1, asphalt binder ages throughout the pavement structures and exhibits a pronounced arc-shaped distribution along the pavement depth; that is, as the pavement depth increases, aging initially decreases and then increases. This phenomenon has also been observed in hundreds of pavement aging profiles from the Long-Term Pavement Performance (LTPP) database [32], further suggesting that the assumption of uniform oxygen and aging distribution in asphalt pavements is inaccurate. These observations point to a fundamental gap: the actual distribution of oxygen and its dynamics within in-service asphalt pavements are not well understood, resulting in inaccurate predictions of pavement aging.

Oxygen distribution inside asphalt pavement is driven by its dynamic behaviors during pavement use and its reaction with asphalt binder, which can be described as follows: 1) oxygen in the air channels of pavements is consumed when reacting with asphalt binder; 2) driven by the oxygen concentration gradient, atmospheric oxygen transports into pavements; 3) boundary interactions at the bottom layers (e.g., unbound/bound layers) of asphalt pavement may act as oxygen sources or barriers, depending on the oxygen content at the boundaries. These oxygen consumption and transport behaviors are intrinsically governed by Multiphysics processes. Specifically, temperature directly influences the consumption and transport rate of oxygen, while moisture can potentially alter thermal behavior and impedes gas transport by occupying the air channels within the pavement. Furthermore, the evolving oxygen distribution field can feed back on the oxidation rate, resulting in a coupled temperature-oxygen-moisture field within in-severing pavements. To simulate the Multiphysics-coupled processes and their impacts on pavement aging, Omairey *et al.* [33,34] developed a Multiphysics aging modelling framework, integrating the oxidative kinetics model [11–15], oxygen transport model [16,35,36], and heat transfer model [37]. Under certain simplified assumptions, their model predicts a C-shaped distribution of oxygen and aging in asphalt pavements with unbound base layers, consistent with the arc-shaped profiles reported in previous studies [27–31]. Although this framework is more mechanistic than the other empirical aging models, its predictive accuracy remains uncertain due to unverified assumptions and a lack of validation against field monitoring data including environmental factors.

While temperature monitoring of in-situ pavements has been performed in several field studies [21–23], long-term in-situ measurement and monitoring of oxygen and moisture in in-service pavements have not been reported. This absence of field data constitutes a significant research gap, likely caused by some technical challenges. In particular, conventional oxygen and moisture sensors cannot withstand the high construction temperatures of asphalt pavements and the subsequent heavy compressive loads. Thus, it is impractical to directly embed the oxygen and moisture sensors within pavements. On the other hand, post-construction installation methods (e.g., coring and backfilling) disrupt the original aggregate skeleton of pavements, creating artificial pathways for air and water that compromise measurement accuracy.

To address this critical gap, this study, for the first time, developed an integrated Multiphysics monitoring system capable of sustained, simultaneous in-situ measurements of temperature, oxygen, and

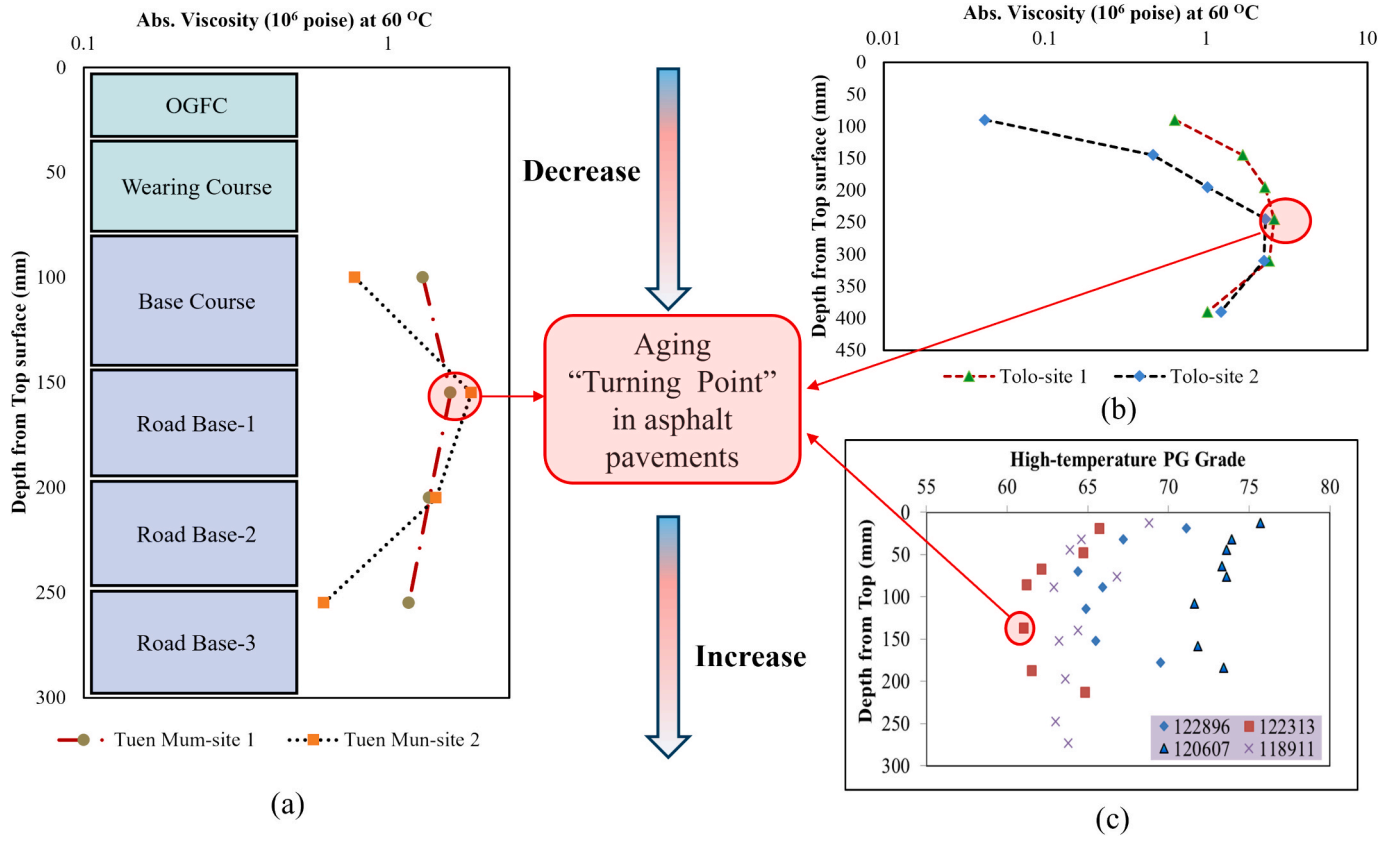

Fig. 1. Aging-depth relationships in three long-life asphalt pavements [25,26]: (a) Tuen Mun Highway, Hong Kong; (b) Tolo Highway, Hong Kong; (c) Pavements in Minnesota.

moisture in asphalt pavements. The system is designed to withstand construction loading and temperature, thereby protecting the sensors and minimizing disturbance to the original aggregate skeleton. Initially, the oxygen measurement module of this Multiphysics monitoring system was employed at the laboratory scale to investigate oxygen distribution in asphalt pavement layers. Laboratory monitoring results highlight the significant impact of mixture design on oxygen distribution within pavements. Subsequently, the entire monitoring system was implemented in a full-scale trial section for field investigations of temperature, oxygen, and moisture at various pavement depths over a year, covering multiple freeze–thaw, dry-wet, and low-low temperature cycles (from January 2024 to December 2024). The resulting dataset provides valuable insights into the pavement's in-service environment, which is crucial for validating and refining the Multiphysics aging modeling framework, contributing to more accurate predictions of aging evolution. The findings are expected to assist in guiding material selection, mixture and structural design, and identifying anti-aging strategies to enhance pavement longevity.

2. The multiphysics measurement system

2.1. Measurement of oxygen

2.1.1. Oxygen collection system

The most accurate method for oxygen concentration measurement within pavement is to embed oxygen sensors directly inside the asphalt layers. However, as aforementioned, most commercial oxygen sensors cannot withstand the high construction temperature of asphalt pavements (above 135 °C), and water leaked into pavements due to heavy rainfall may lead to the failure of oxygen sensors. These factors are the primary reasons for the scarcity of field oxygen data in asphalt pavements. Additionally, oxygen concentration in asphalt pavements is highly sensitive to the surrounding volumetric properties of the asphalt mixture. If oxygen sensors are installed using a coring-burying-backfilling approach, variations in the volumetric properties of the surrounding asphalt mixture can significantly affect the precision of oxygen measurements.

To address these challenges, this study developed an oxygen collection system designed to extract in-situ air samples for remote oxygen concentration analysis. As illustrated in Fig. 2, the system consists of an outer Polyetheretherketone (PEEK) tube and inner Teflon pipelines, with the gap between the PEEK tube and Teflon pipelines sealed using asphalt binder to prevent oxygen leakage. The airtightness of the entire air sampling system was rigorously verified in the laboratory prior to deployment. Specifically, the system was pressurized with 100% nitrogen, and oxygen levels within the pipeline were monitored continuously for over one month. The results confirmed excellent airtightness, with oxygen content variation remaining below 0.1%. Therefore, the airtightness of the air sampling system is highly reliable. Moreover, there might be a time lag of oxygen concentration between the sampling point within the pavements and the oxygen sensor. To evaluate system responsiveness, we performed a simulation experiment. By introducing nitrogen into a sealed chamber connected via our sampling tube, we created a rapid drop in oxygen concentration. The sensor at the opposite end recorded a stabilization of readings within minutes of the chamber's gas change, demonstrating that the system's intrinsic response time to a concentration shift is relatively short. Furthermore, PEEK is a thermoplastic engineering plastic known for its excellent physical and mechanical properties. Thus, the primary function of PEEK tube is to protect the inner Teflon pipelines. Compared to traditional metal protection tubes, PEEK presents better chemical stability and flexibility, which helps minimize interference with the original pavement environments.

2.1.2. Oxygen sensors

The oxygen collection system was then connected to oxygen sensors for the measurement of oxygen in asphalt mixtures and subsequently asphalt pavements. Specifically, a high-precision galvanic cell oxygen sensor, Apogee SO-210, was employed for the oxygen measurement in this study. The principal working mechanism of this sensor relies on the proportional relationship between electricity current flow and the absolute concentration of oxygen diffusing through the membrane.

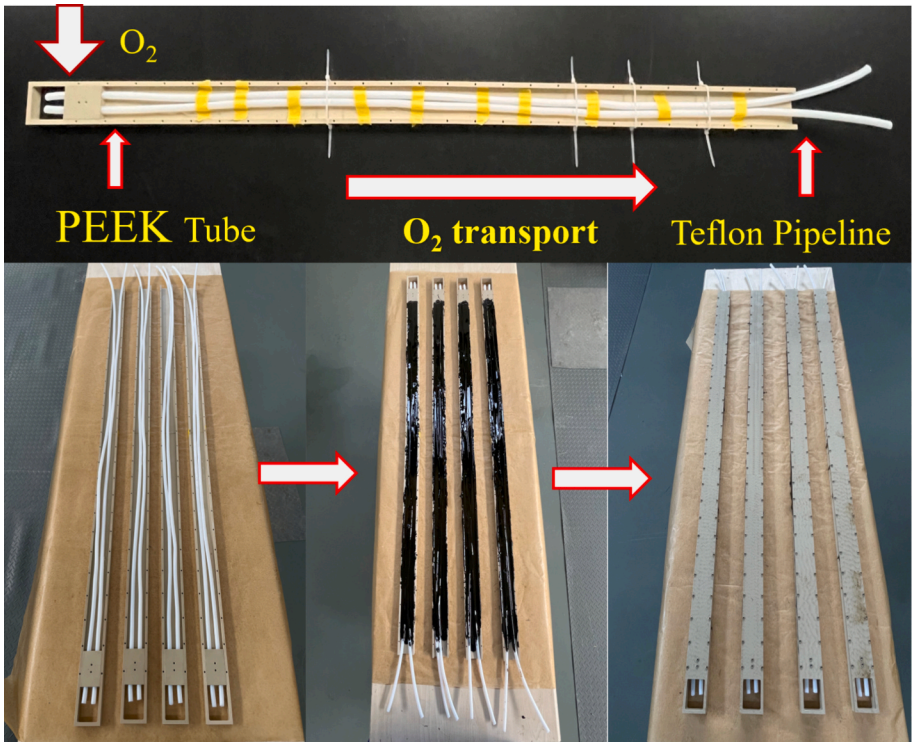

Fig. 2. The oxygen collection system.

Accordingly, the recorded current flow was used to determine oxygen concentrations. The specifications of the Apogee SO-210 sensor are provided in Table 1.

2.2. Measurement of temperature and moisture

Temperature and moisture are the other two key factors influencing the oxygen consumption and transport behaviors, ultimately affecting the distribution of oxygen in asphalt pavements. Thus, a composite temperature-moisture sensor, SMT 100, was used to measure both temperature and moisture content in the trial section. The specifications of the SMT 100 are provided in Table 2. However, similar to the Apogee SO-210, the operational temperature range of the SMT 100 restricts its direct installation during pavement construction. To overcome this limit, a customized PEEK protection tube was first embedded in the asphalt pavement during construction, allowing for the subsequent installation of the SMT 100 sensor.

Additionally, since the moisture measurement function of SMT 100 was originally designed for soil, it requires full contact between the probe and the surrounding material. However, different than soil, asphalt concrete layers contain large air gaps, which may affect the accuracy of moisture measurements using the SMT 100. To minimize this impact, loose asphalt mortar composed of asphalt binder and standard sand (particle size 0.08–2.00 mm) was used to fill the air gaps between the SMT 100 and asphalt concrete layers. Initially, loose asphalt mortar was pre-placed in the collection window of the protection tubes. After pavement construction with embedded tubes, the SMT 100 sensor was fully inserted into the asphalt mortar, and any remaining gaps between the sensor and the tube were filled with additional loose asphalt mortar to ensure complete contact. The preparation of temperature-moisture sensors and their protection tubes is illustrated in Fig. 3.

Furthermore, the SMT 100 sensor is calibrated for soil, and that the dielectric constant of loose asphalt mortar differs from that of soil. Therefore, we did not use the raw output from the SMT 100 to directly represent the true, absolute volumetric water content (VWC) of the asphalt mortar. Instead, we used the sensor as a sensitive and stable dielectric probe to track relative changes in the moisture condition within the mortar. Thus, a relative moisture (%) index was defined (ratio of current reading to saturated reading) for the identification of moisture conditions across different pavement layers, which was shown in Eq. (1):

$$relativemoisture(\%) = \frac{measuredVWC}{maximumVWC} \times 100\% \quad (1)$$

Here, which is a critical reference point established through a controlled laboratory procedure. It is not a true measurement of VWC for asphalt mortars, but rather the SMT 100 sensor's raw output reading (in % VWC units as per its soil calibration) when the asphalt mortar sample is in a saturated state. The laboratory testing procedure was as follows: 1) A standard SMT 100 sensor was fully embedded in a representative sample of the same loose asphalt mortar used in the field. The sensor was centered in a protective tube, and all gaps were meticulously filled with additional mortar to ensure full, homogeneous contact, mimicking the field installation. 2) The prepared sample was placed on a tray. Water was slowly and carefully added to the tray, allowing it to infiltrate the mortar from the bottom upwards. 3) The SMT 100 reading was logged continuously. Water was added until the sensor reading stabilized, indicating no further water could be absorbed into the mortar's accessible voids under this setup. This stabilized maximum reading was approximately 38% on the sensor's display (which is scaled for soil). As a result, the relative moisture basically reflects the percentage of air voids filled with water, providing a comparative measure of moisture conditions in various pavement layers, even though it does not represent the ture moisture content.

Table 1
The specifications of the oxygen sensor Apogee SO-210.

Description	Value
Operating temperature	−20 to 60 °C
Operating relative humidity	0 to 100%
Measurement Range (O_2)	0 to 100%
Response Time (time required to read 90% of saturated response)	14 s
Dimensions	32 mm diameter, 68 mm length
Flow Through Head	35 mm diameter 86 mm length

Table 2
The specifications of the temperature-moisture sensor SMT 100.

Description	Value
Range temperature measurement	−20 to 85 °C
Resolution temperature measurement	0.01 °C
Range temperature measurement	0 to 100% Volumetric Water Content (VWC)
Resolution soil moisture measurement	0.1% VWC
Total length of sensor	182 mm
Length of moisture measurement field	113 mm
Length of temperature measurement field	69 mm

2.3. The integrated field monitoring system

The integrated field monitoring system consisted of the oxygen collection system, protection tubes for the temperature-moisture sensors, and a customized stainless-steel box, as illustrated in Fig. 4. The customized stainless-steel box served two primary functions: (1) to prevent unexpected movements of the oxygen collection system and protection tubes during the pavement compaction process. (2) to position the oxygen collection system and protection tubes at critical depth within the trial section using specially designed slots. With the assistance of this field sampling system, oxygen, temperature, and moisture can be accurately measured at designated locations within the asphalt pavement.

2.4. Data acquisition and wireless transmission system

The measured data of oxygen, temperature, and moisture were collected and transmitted using an integrated data acquisition and wireless transmission system, comprising a data logger and wireless transmission modules. Sensor outputs were initially recorded by a commercial data logger (Campbell CR1000X) at five-minute intervals. These electrical signals were then processed and converted into oxygen concentration, temperature, and volumetric water content (VWC) readings using LoggerNet, a communication software compatible with the Campbell CR1000X. Subsequently, the processed data was transmitted and stored on a cloud platform via the BOR-D401S wireless transmission module, developed by Comway IOT Communication Corp. This setup enabled real-time monitoring and remote access to the collected data.

3. Laboratory and field measurement methods

3.1. Materials

Three types of asphalt mixtures, SMA-13, AC-20, and ATB-25 were prepared for the construction of the asphalt pavement trial section, following the Chinese technical specification JTG F 40. The gradation designs for these mixtures are illustrated in Fig. 5. For the SMA-13 mixture, basalt aggregate was combined with 3% fiber and 6% commercial modified asphalt binder. AC-20 and ATB-25 mixtures were produced using limestone aggregate and XinHai-70# base asphalt binder, with binder contents set at 4.3% and 3.6%, respectively. Table 3

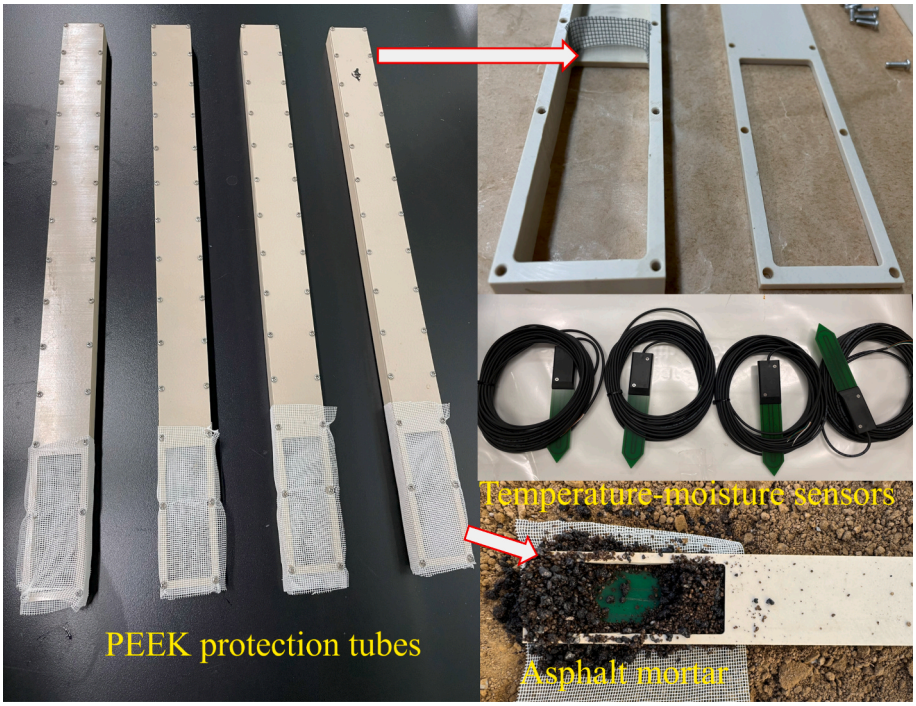

Fig. 3. The temperature-moisture sensors and their protection tubes.

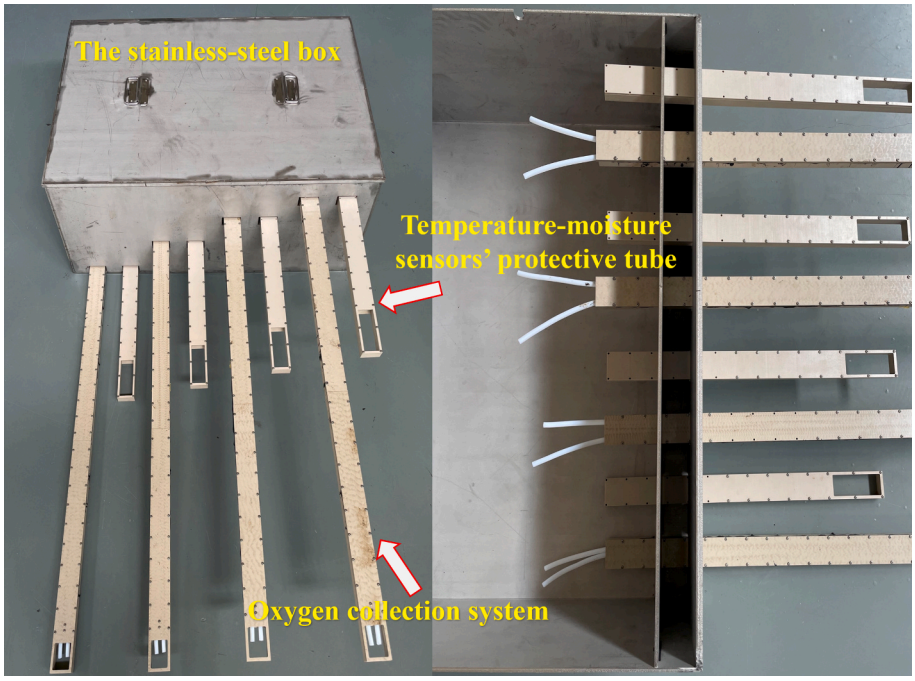

Fig. 4. The field sampling system.

summarizes the properties of the commercial modified asphalt binder and the XinHai-70# base binder. The measured air voids for the SMA-13, AC-20, and ATB-25 mixtures were 4.8%, 5.0%, and 4.8%, respectively. Additionally, slab samples of AC-20 and SMA-13 were prepared in accordance with AASHTO T 324 specifications for laboratory measurement of oxygen in single asphalt concrete layers.

3.2. Laboratory measurement of oxygen in single asphalt concrete layers

The existing Multiphysics aging modeling framework [33,34] employs a statistical function to predict the oxygen diffusion coefficient of asphalt mixtures based on air void content, assuming that higher air voids correspond to faster oxygen supply. However, recent studies [16–18] have shown that increased air void content does not necessarily result in a higher oxygen transport rate, and the statistical function is only applicable to asphalt mixtures with the same mixture design. To investigate the effect of mixture design on oxygen distribution within asphalt concrete layers, laboratory-scale slabs of SMA-13 and AC-20 were prepared using a custom mold specifically designed for oxygen measurement. The mold measured 305 mm in length and width, with a

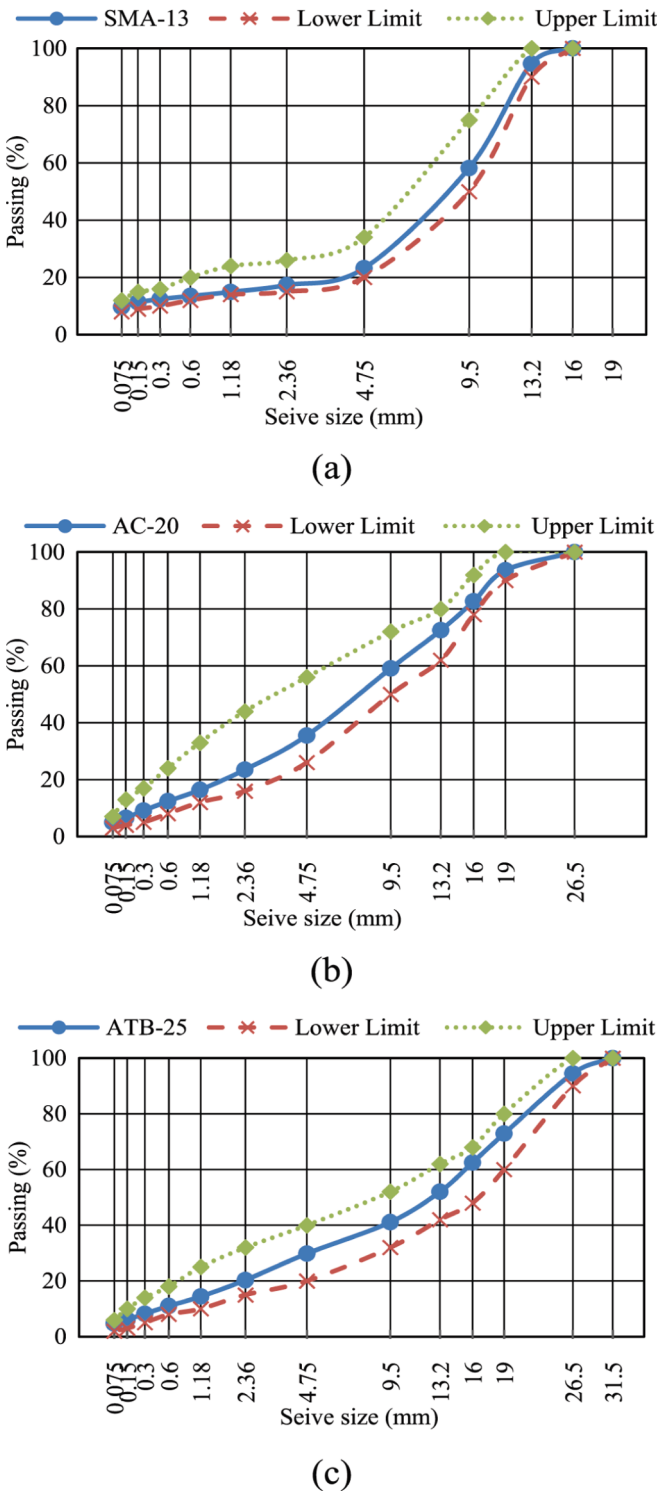

Fig. 5. Aggregate gradation: (a) SMA-13; (b) AC-20; (c) ATB-25.

height of 80 mm—30 mm taller than the slabs typically used for the Wheel-Tracking test. A rectangular groove (45 mm wide and 20 mm high) was constructed at the bottom of one side panel of the mold to accommodate the oxygen collection system, resulting in an oxygen measurement depth of approximately 60 mm below the top surface of the asphalt mixture. The slab samples were compacted using a rolling compaction machine, and silicone sealant was applied to all joints around the mold to prevent oxygen exchange through any gaps. The prepared samples were then connected to the data acquisition and wireless transmission system for continuous measurement and monitoring of oxygen concentrations. The laboratory sample preparation process and the oxygen monitoring system are illustrated in Fig. 6.

Table 3
The properties of modified binder and XinHai-70# base asphalt.

Description	Unit	Modified binder	XinHai-70# base asphalt	Specification
Specific Gravity (15 °C)		1.035	1.036	ASTM D70
Penetration (25 °C)	0.1 mm	63	67	ASTM D5
Softening point	°C	76.5	48	ASTM D36
Ductility	cm	36 (5 °C)	34 (10 °C)	ASTM D113
Flash point	°C	254	268	ASTM D 92
Retained penetration percentage after the thin-film oven Test (25 °C)	%	67.9	67.4	ASTM D5
Ductility after the thin-film oven test	cm	22.3 (5 °C)	6.8 (10 °C)	ASTM D113

3.3. Field measurement of oxygen, temperature, and moisture

3.3.1. Site conditions

A trial section of asphalt pavement, measuring 4 m × 6 m × 0.46 m, was constructed at the National Center for Materials Service Safety in Beijing for the field measurements and long-term monitoring of oxygen, temperature and moisture content. This site is located in a temperate continental monsoon climate zone, characterized by hot-rainy summers and cold-dry winters [38]. The pronounced seasonal climate variations in Beijing are expected to provide comprehensive data on pavement environmental conditions. Fig. 7 presents the pavement structures of the trial section, where a 40 mm wearing course (SMA-13), 60 mm base course (AC-20), and 180 mm road base (ATB-25) were laid over a 180 mm subgrade composed of soil with 95% compaction. Considering that the excessive thickness of ATB-25 layer might challenge the compaction quality, one 100 mm ATB25-2 layer was initially paved over the subgrade, followed by an additional 80 mm layer of ATB25-1.

3.3.2. The layout of measurement positions

As aforementioned, the field sampling system was employed to measure oxygen, temperature, and moisture at the bottom of each pavement layer. Accordingly, the measurement depth in the trial section was 40 mm, 100 mm, 180 mm, and 280 mm, respectively. The layout of the measurement positions is illustrated in Fig. 8. To mitigate the impact of potentially low compaction quality near curbs on measurement accuracy, the temperature-moisture sensors and oxygen sensors were positioned 0.55 m and 1.55 m away from the curb, respectively. Furthermore, to minimize interference between the oxygen collection systems and protection tubes during data collection, they were spaced 50 mm apart, ensuring that only one oxygen collection system or protection tube was present along the same vertical line.

3.3.3. Site construction

Prior to the construction of pavements, a working well was constructed to accommodate the placement of the stainless-steel box. The surrounding gaps between the box and working well were filled with grouting cement, and after curing, the box was sufficiently reinforced to serve as part of the curb during pavement construction. The construction process began with soil compaction, ensuring a compact rate exceeding 95%. Next, the oxygen collection system and the protection tubes for the temperature-moisture sensors were positioned on the soil surface and inserted into the bottom slots of the stainless-steel box for secure placement. Subsequently, the asphalt concrete layers, along with the oxygen collection system and protection tubes, were paved layer by layer. Meanwhile, several comprehensive approaches were taken to ensure uniform compaction around the embedded sampling systems and eliminate preferential pathways for air and water. For instance, a

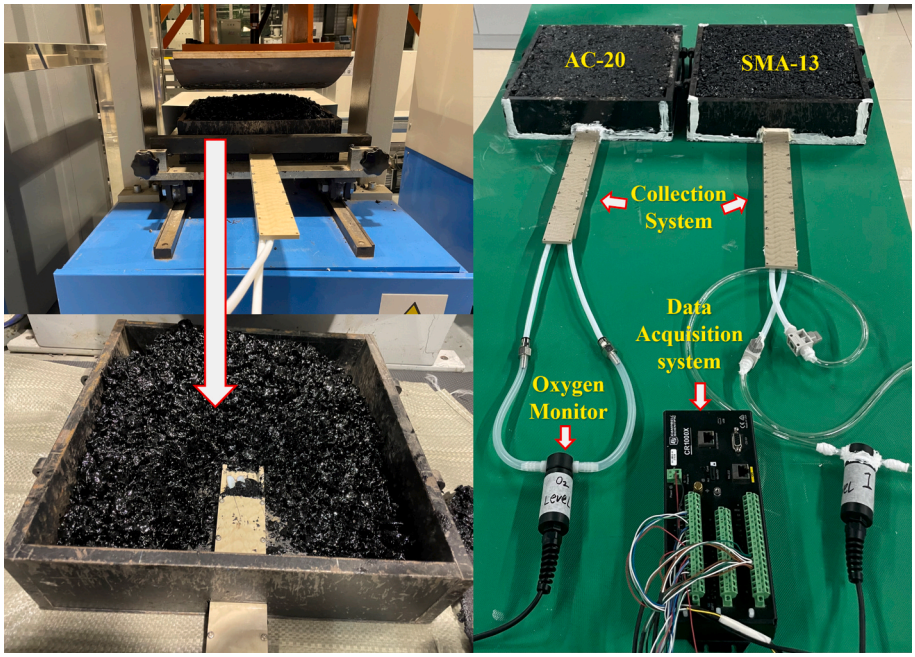

Fig. 6. Laboratory measurement of oxygen in asphalt concrete layers.

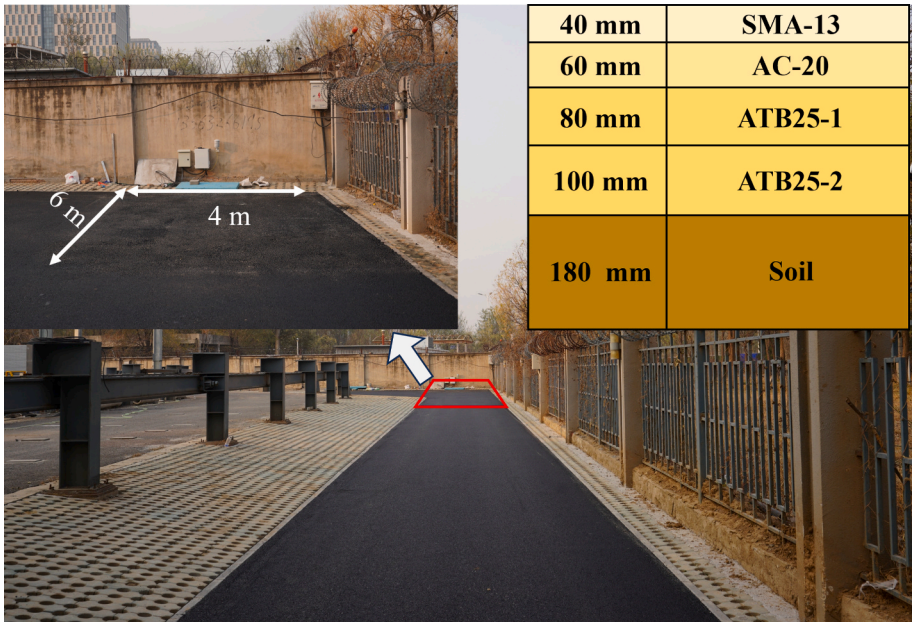

Fig. 7. The trial section of asphalt pavements.

sequenced compaction strategy was employed to guarantee intimate contact between the asphalt and the sampling systems' walls. Specifically, prior to the full width rolling of the asphalt layer, hot mix asphalt was manually placed around each sampling system. A vibratory plate compactor was then used to perform targeted, manual compaction in these specific areas. This critical step ensured initial densification and eliminated potential "bridging" of aggregates around the sampling systems. Following this localized treatment, standard full-scale pavement compaction was carried out sequentially using a steel-wheel roller, a pneumatic tire roller, and finally a small steel-wheel roller. This standard sequence ensured that the locally pre-compacted zones were seamlessly integrated into the uniformly compacted pavement layer. Upon completion of the pavement layers, the gaps between the fixing slabs within the stainless-steel box were filled with cement to prevent water and air infiltration. Finally, the field monitoring system was connected to the data acquisition and wireless transmission system, enabling real-time measurement and monitoring of oxygen, temperature, and moisture at various depths within the asphalt pavement section. The field construction process and monitoring system layout are illustrated in Fig. 9.

4. Results and discussion

4.1. Laboratory monitoring results of oxygen in asphalt mixtures

Fig. 10 presents the results of a four-month laboratory monitoring of oxygen concentration at the bottom of SMA-13 and AC-20 asphalt mixtures, respectively, alongside room temperature and ambient air

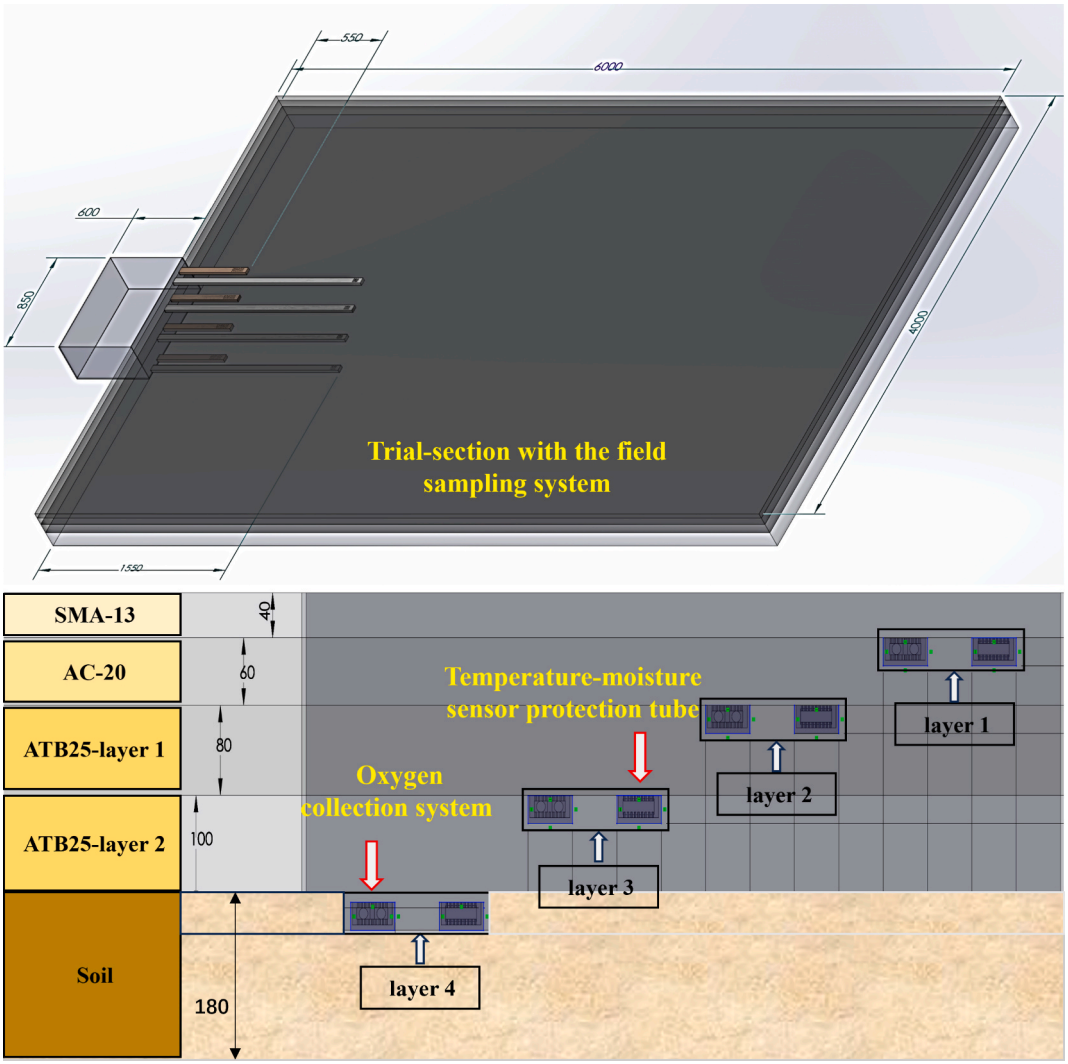

Fig. 8. The layout of the field monitoring system.

oxygen concentration. The monitoring started on June 7 and ended on October 7, 2023. Due to unexpected power supply issues in the laboratory, data were not recorded during two periods: July 12 to August 17 and September 5 to September 21. These gaps are indicated by dashed points in Fig. 10. Fortunately, these interruptions did not significantly affect the overall trends observed in the oxygen concentration data for the asphalt mixtures.

In Fig. 10, the oxygen concentration curve for AC-20 presented a nearly consistent trend with the ambient oxygen concentration curve, and their oxygen concentrations remained at similar levels throughout the monitoring period. This suggests that the rate of oxygen transport in AC-20 enabled rapid replenishment of consumed oxygen from the ambient air. In contrast, the oxygen concentration in SMA-13 exhibited a distinctly different pattern: it dropped sharply at the beginning of the monitoring period, and then stabilized at approximately 18.5% for an extended duration. When the room temperature decreased noticeably in September, the oxygen concentration in SMA-13 gradually increased, eventually reaching around 19.7%. This behavior can be explained as follows: (1) Initially, oxygen was consumed at the bottom of SMA-13, but the slow oxygen transport rate prevented rapid replenishment of oxygen from the atmosphere, resulting in a rapid decrease in oxygen concentration; (2) Over time, a dynamic equilibrium was established between the slow rates of oxygen supply and consumption, leading to prolonged stabilization; (3) As room temperature dropped, the rate of oxygen consumption decreased, causing the oxygen concentration to rise.

According to the oxygen transport model used in the Multiphysics oxidative aging model, SMA-13 and AC-20, with similar air voids (around 5%), would be expected to have similar oxygen diffusion capacity and, consequently, similar oxygen distribution profiles. However, the laboratory monitoring results clearly indicate that this is not the case. In fact, according to a previous study [17], the oxygen diffusion coefficient of AC-20 was more than 15 times greater than that of SMA-13, when their air voids were around 5%. This discrepancy may be attributed to the difference in volumetric properties between SMA-13 and AC-20, where AC mixture is characterized by numerous small and interconnected air voids, while the SMA mixture is dominated by larger and isolated air voids. More interconnected air voids in AC-20 lead to faster supplementation of oxygen than SMA-13. These findings suggest that the quantitative relationship between air voids and oxygen diffusion coefficient, as currently proposed in the Multiphysics oxidative aging model, requires further refinement.

4.2. *Field monitoring results of temperature in the trial section*

The field monitoring results of temperature in the trial section are presented in Fig. 11, revealing a typical seasonal variation characteristic: temperatures are lower in winter and higher in summer. However, an anomaly was observed between July 12 and July 20, when pavement temperature dropped sharply and remained at that level similar to air

Fig. 9. The field construction process and the layout of the monitoring system.

temperatures. This period coincided with persistent heavy rainfall in Beijing, which escalated into severe flooding and then submerged the entire trial section. The inconsistent temperature readings during this time are attributed to the immersion of the pavement in water.

Despite this exceptional event, the pavement temperature profiles exhibited regular trends. Several phenomena can be observed: (1) The variation of daily temperature decreased with the increase of pavement depth. (2) A temperature swing can be observed in the daytime and at night. As illustrated in Fig. 12, pavement temperatures at 12:00 pm and 00:00 am showed different distributions. During the day, temperatures decreased from the SMA layer to the ATB-2 layer, while at night, temperatures decreased from the ATB-2 layer to the SMA layer. This resulted in the largest daily temperature variation occurring in the top layer and the lowest variation of daily temperature in the bottom layer. Furthermore, the daytime temperature contributes more to the oxidative aging of asphalt binders than the nighttime temperature since the daytime temperature is much higher than the nighttime temperature. As a result, the field temperature monitoring results support the conventional assumption of unidirectional attenuation of aging with depth, if not accounting for the effects of oxygen distribution.

4.3. Field monitoring results of moisture in the trial section

Fig. 13 presents the field monitoring results of relative moisture at the bottom of different pavement layers. In this context, 100% relative moisture represents a saturated condition, while 0% indicates the complete absence of water in the asphalt pavements. Among the monitored layers, the ATB25-2 layer exhibited distinct characteristics, with higher and more fluctuating relative moisture values compared to the others. This difference can be attributed to the fact that the bottom of the ATB25-2 layer consists of soil, which is more sensitive to changes in ambient water conditions than asphalt concrete. Soil allows water to enter and escape more easily, making it prone to rapid saturation during heavy rainfall events and quick drying once the rain stops. In this study, the soil moisture quickly returned to its regular state value (around 24%) after intense precipitation events, resulting in pronounced peaks in the relative moisture curve for ATB25-2.

Furthermore, the relative moisture results for the trial section can be divided into three distinct phases. Phase One (January to May): During this period, the relative moisture at the bottom of the SMA-13, AC-20, and ATB25-1 layers remained extremely low. Phase Two (June to September, Flood Season): With the start of the rainy season, frequent and intense precipitation caused a significant increase in relative moisture across all layers. Notably, the relative moisture in the AC-20 and ATB25 layers occasionally approached 100% before returning to normal levels, while the SMA-13 layer consistently maintained a low moisture level. This phenomenon suggests that heavy rainfall led to the saturation of the AC-20 and ATB25 layers, whereas the superior waterproofing performance of the SMA-13 layer effectively prevented the entry of water. Phase Three (September to December): After the rainy season, as Beijing transitioned into a cold and dry winter, the relative moisture in the asphalt concrete layers remained stable and did not return to the low levels observed in Phase One. This may indicate that, although water could infiltrate the asphalt pavement under persistent heavy rainfall, it was difficult for it to escape. The long-term existence of water was detrimental to the performance of asphalt pavements. Thus, further measurements and analysis of moisture are needed to better understand the water environment in asphalt pavements.

4.4. Field monitoring results of oxygen concentration in the trial section

4.4.1. The time-series trends of oxygen concentration

The time-series trends of oxygen concentration in the trial section are

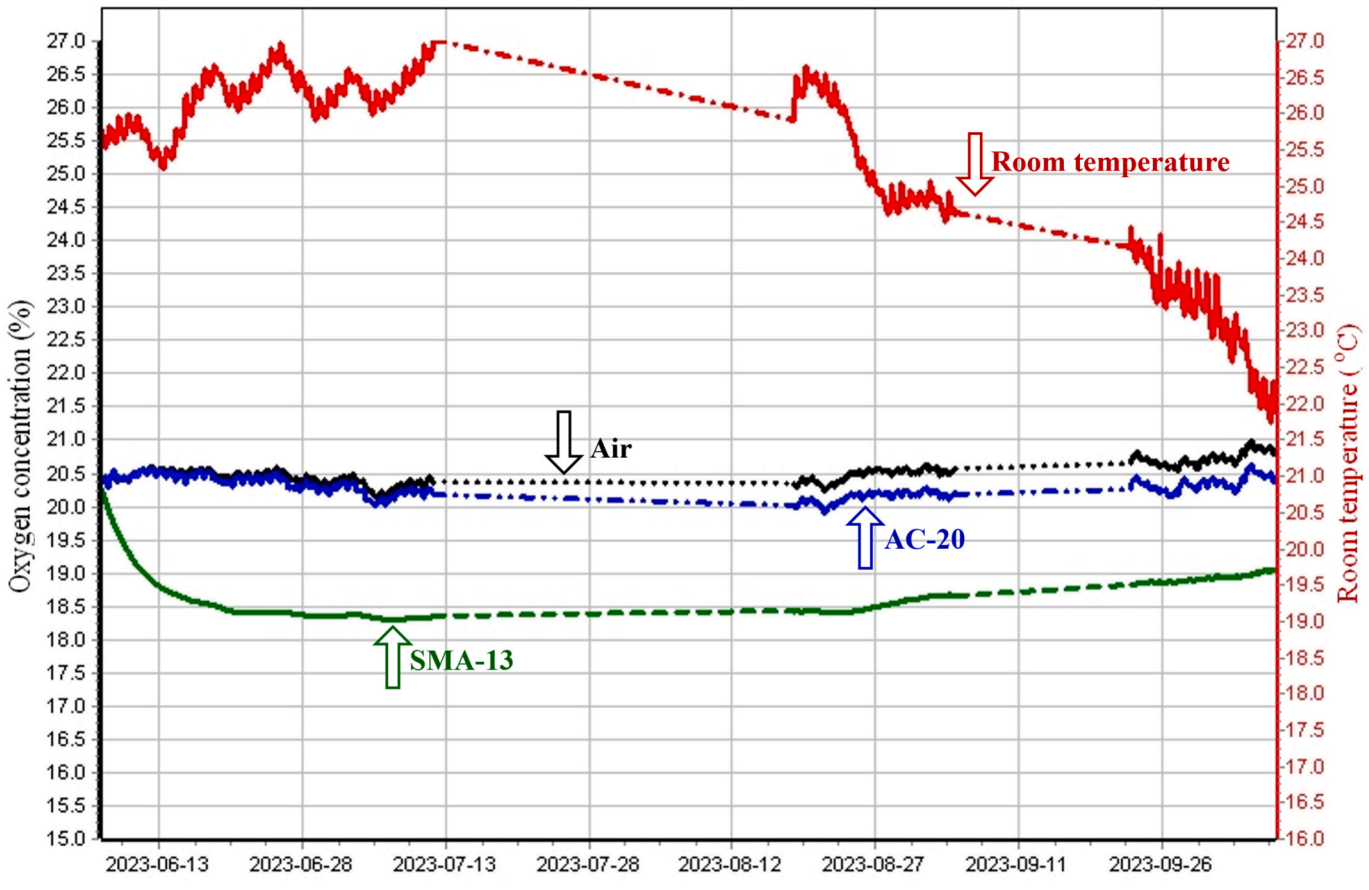

Fig. 10. Laboratory monitoring results of oxygen concentrations in SMA-13 and AC-20.

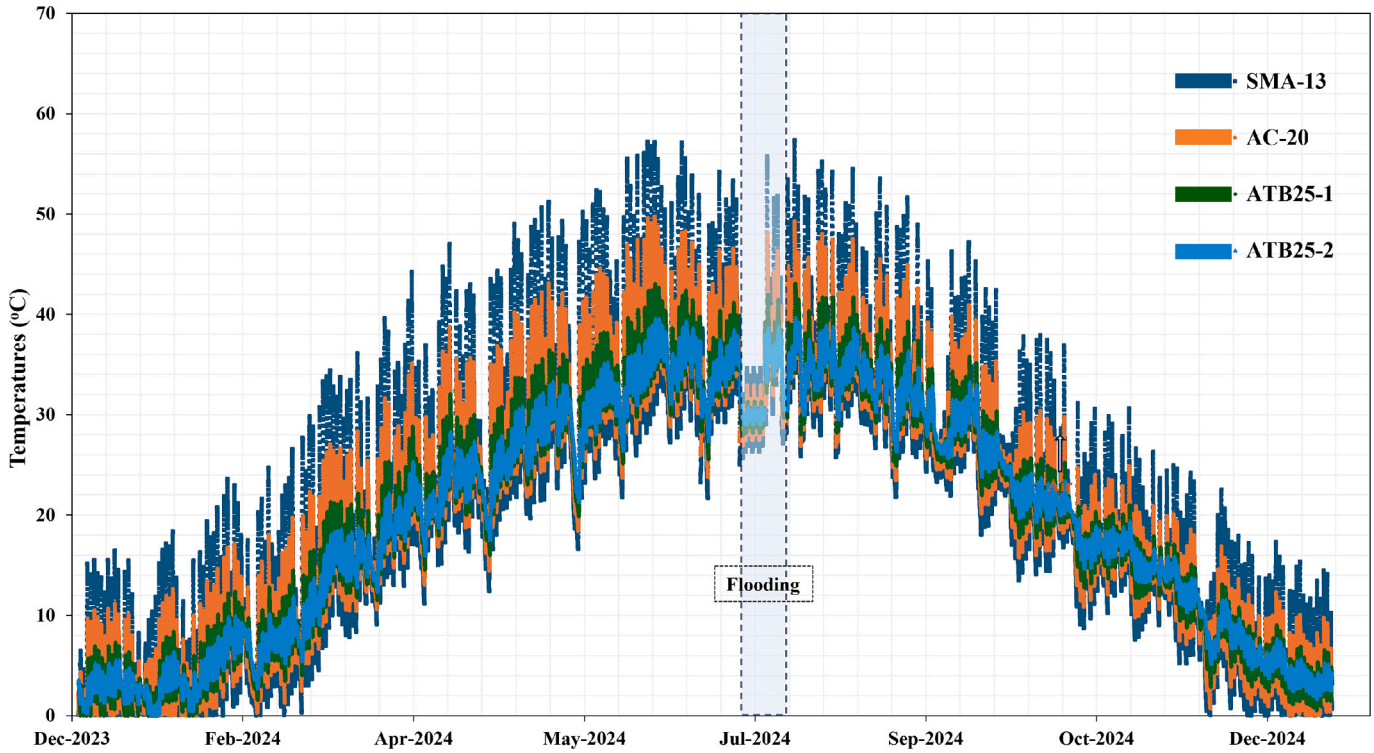

Fig. 11. Field monitoring results of temperature in the trial section.

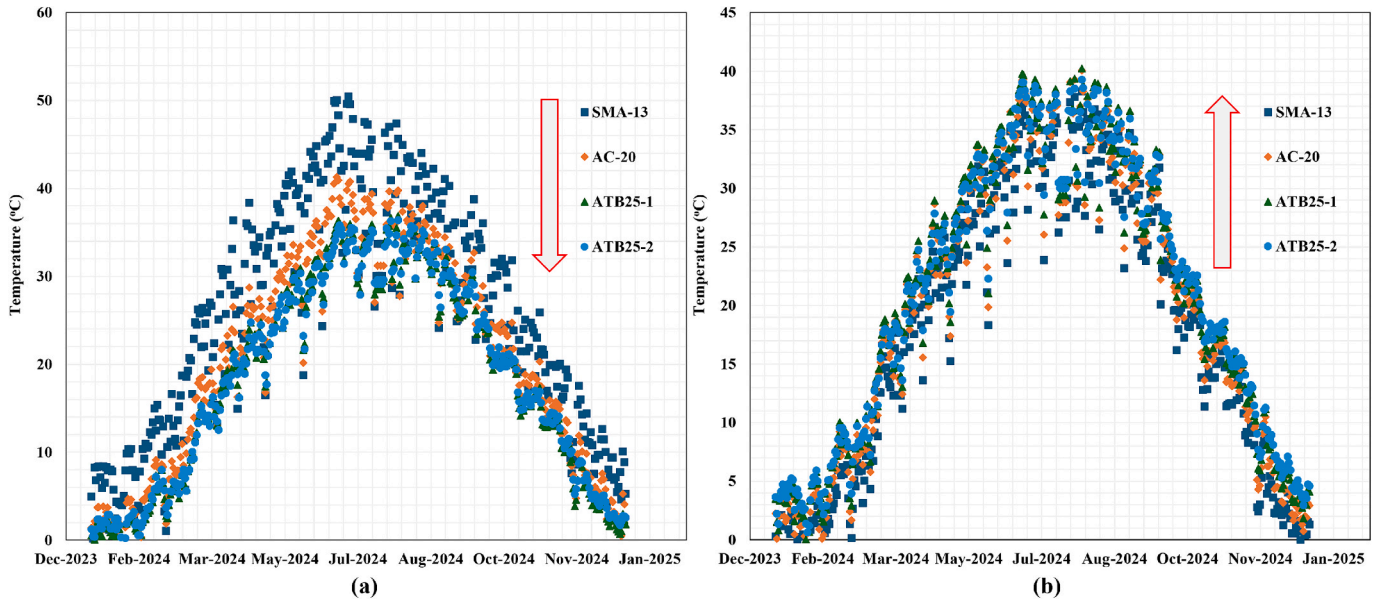

Fig. 12. Daytime temperature and nighttime temperature in the trial section: (a) temperature at 12:00 pm; (b) temperature at 00:00 am).

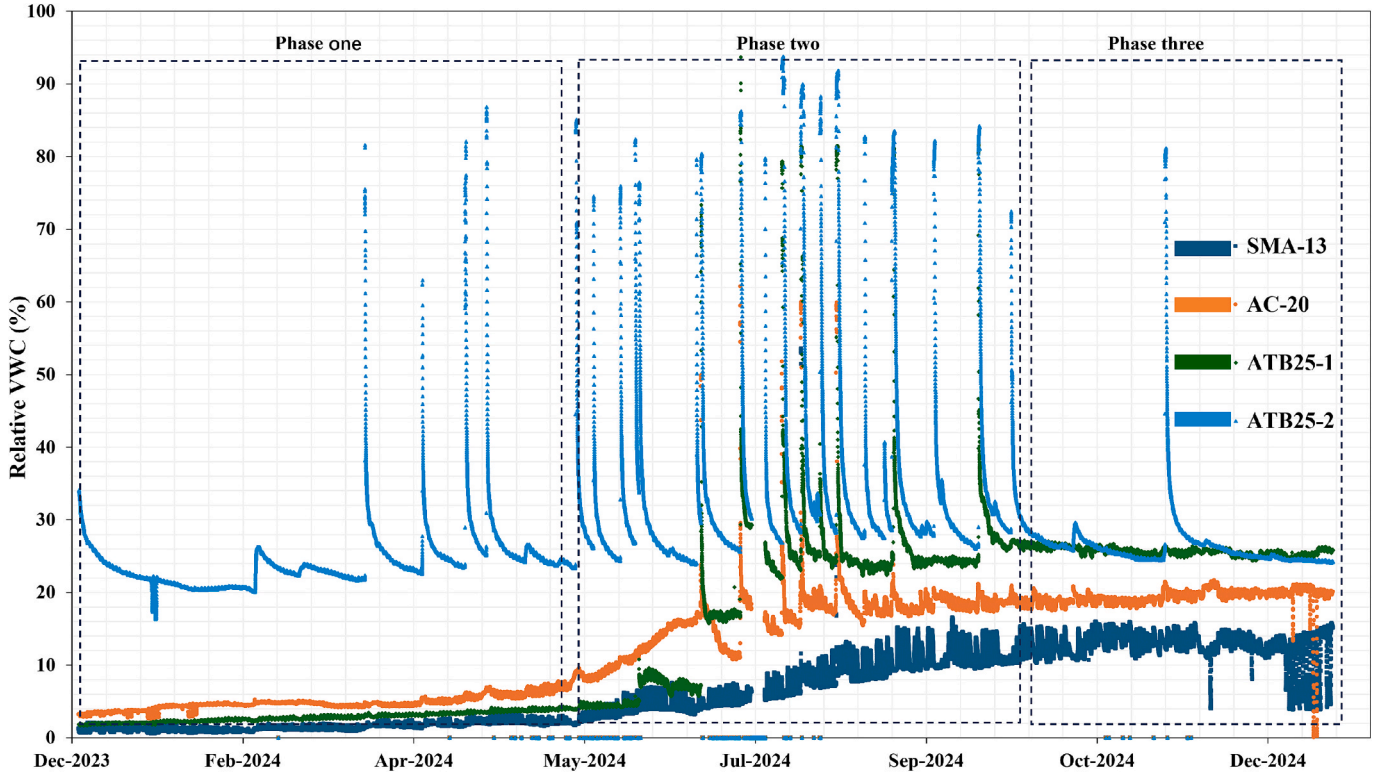

Fig. 13. Field monitoring results of relative moisture in the trial section.

presented in Fig. 14. Similar to the relative moisture results, the variation in oxygen concentration exhibits three distinct phases. In Phase One (January to June), oxygen concentration in each pavement layer gradually decreased, primarily due to increased oxygen consumption resulting from rising pavement temperatures. During the period of persistent intense precipitation (July to August), oxygen concentration in the trial section fluctuated drastically. Notably, oxygen levels at the bottom of the ATB25-2 layer (i.e., the soil subgrade) dropped sharply to zero. The trial section was entirely submerged due to unexpected heavy rainfall. Because prolonged water immersion could affect the accuracy of the oxygen sensors, monitoring was temporarily suspended from July 15 to August 8. After this period, as rainfall intensity and frequency decreased, the oxygen sensors were reconnected to resume measurement. In the third phase, as pavement temperatures declined, the rate of oxygen consumption decreased, resulting in gradually increasing oxygen concentrations in each layer, eventually approaching atmospheric levels.

4.4.2. The depth profile of oxygen concentration

Fig. 15 illustrates the monthly average oxygen concentration at the

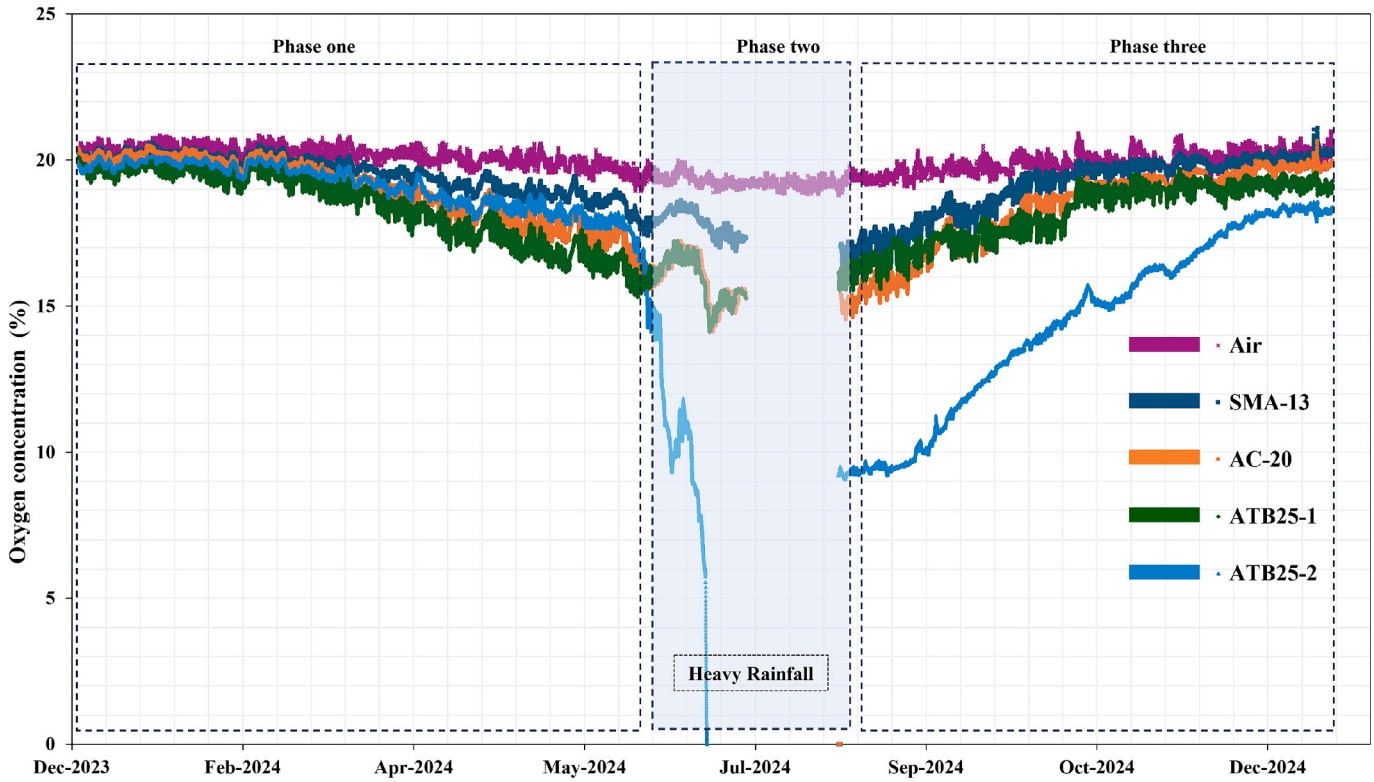

Fig. 14. Field monitoring results of oxygen concentration in the trial section.

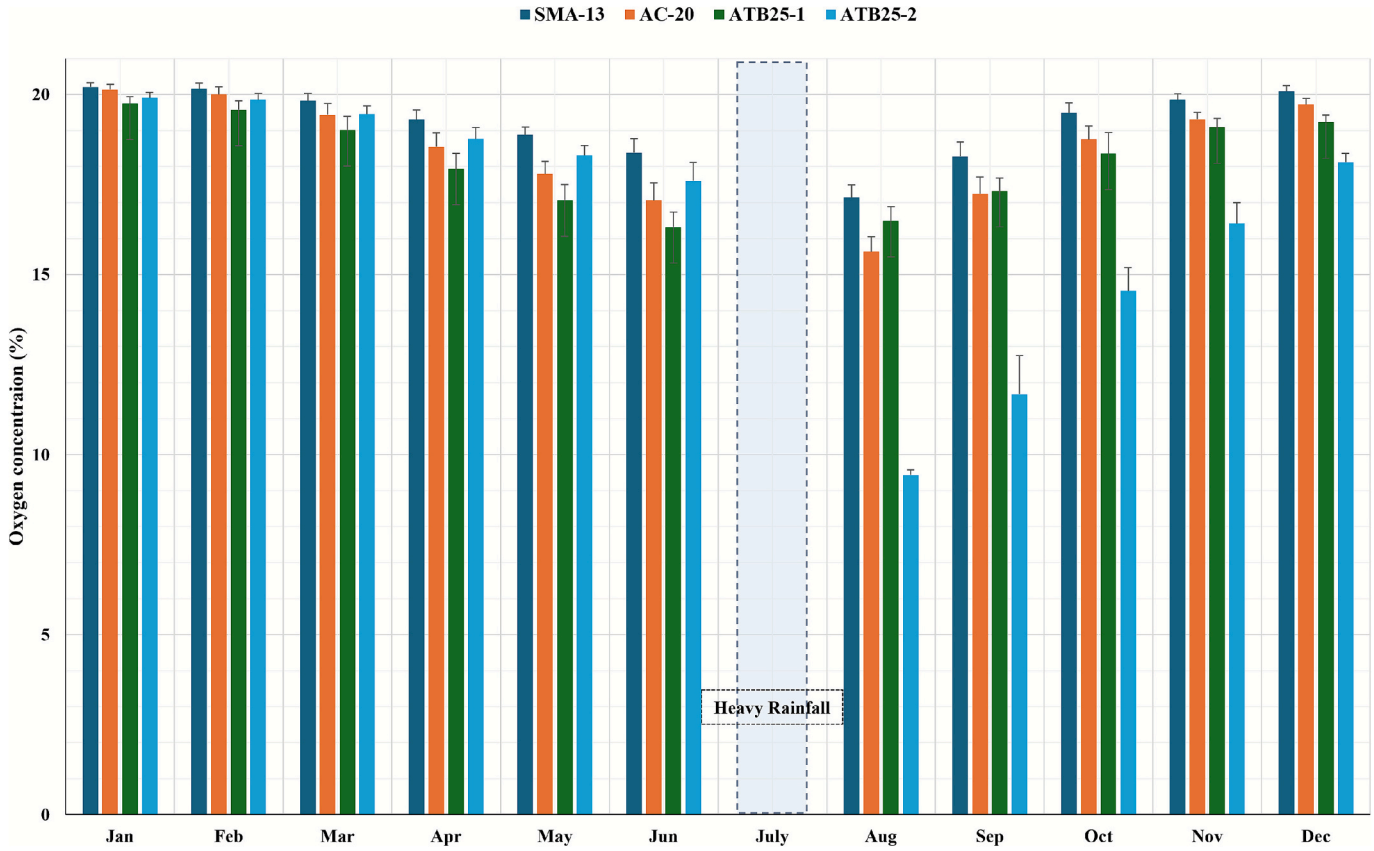

Fig. 15. Monthly average oxygen concentration in the trial section.

bottom of each pavement layer, excluding July when data were unavailable due to heavy rainfall. Subsequently, the depth profile of

oxygen concentration are divided into two distinct periods based on observed oxygen distribution patterns: January to June (Fig. 16a) and August to December (Fig. 16b). During the first period (January to June, Fig. 16a), oxygen concentration consistently decreased from the surface SMA-13 layer to the ATB25-1 layer, and then increased in the ATB25-2 layer. This trend became increasingly pronounced over time and aligns with previously discussed pavement oxidative aging profiles. Moreover, this observation contradicts the common assumption that oxygen levels in unbound asphalt pavements either decrease or remain at atmospheric levels. After the flooding period, the oxygen distribution pattern shifted. As shown in Fig. 16b (August to December), oxygen concentration decreased from SMA-13 to AC-20, increased at ATB25-1, and then dropped again in ATB25-2. The abnormally low oxygen concentration in the soil (ATB25-2) may be attributable to saturated subgrade soil conditions. As subgrade soil gradually loses moisture in the autumn and winter months, the oxygen level in the soil is also recovered, which further affects the oxygen content variation in the asphalt mixture adjacent to the subgrade soil.

4.4.3. *A bidirectional model explanation*

A bidirectional oxygen diffusion model is proposed to explain the initial decrease and subsequent increase in oxygen concentration observed in Fig. 16a. As illustrated in Fig. 17, oxygen within pavement pores is consumed through oxidation reactions with asphalt, creating an oxygen concentration gradient that drives atmospheric oxygen to diffuse into the pavement. Simultaneously, oxygen in the roadside soil is depleted by the respiration of plant roots and microbial activities, causing atmospheric oxygen to diffuse into the soil layer as well. For the typical roadside soil at our test site, with an estimated air-filled porosity ranging between 5% and 30%, the predicted oxygen diffusion coefficient for the soil falls within the range of approximately 10^{-2} to 10^{-4} cm^2/s according to classic diffusion models for porous media [39,40]. Meanwhile, the oxygen diffusion coefficient for the asphalt layers in this trial section is in the order of 10^{-4} to 10^{-5} cm^2/s which can be tested using the equipment developed in previous studies [16,17]. Therefore, the oxygen diffusion coefficient in unsaturated soil is approximately 10 to 100 times greater than that in asphalt mixtures. Consequently, at the interface between the ATB25 and the soil layer, the oxygen concentration in the soil layer is higher than that in the ATB25 layer. Driven by the concentration gradient, oxygen from the soil layer diffuses upward into the pavement until equilibrium is reached at a certain depth.

This bidirectional oxygen diffusion model explains the observed pattern in the trial section, where oxygen concentration initially decreases and then increases with pavement depth. However, in reality, the oxygen exchange process between pavement and soil layers is more complex. Factors such as lateral oxygen exchange, soil moisture content, and seasonal variations in plant and microbial respiration further influence this process. Thus, additional studies are needed to better elucidate the mechanisms of oxygen transport and distribution in the entire asphalt pavement structure.

5. Conclusion and recommendations

This study developed and implemented comprehensive laboratory and field monitoring systems to investigate the spatial and temporal distribution of oxygen, temperature, and moisture in asphalt pavements, to advance the understanding of pavement oxidative aging mechanisms. The following conclusions are drawn from the measuring and monitoring results.

(1) Laboratory monitoring results revealed that oxygen transport and distribution in asphalt mixtures are not solely determined by air void content, but are also significantly influenced by the connectivity and morphology of the void structure. Specifically, AC-20 mixtures with more interconnected air voids replenished the consumed oxygen faster than the SMA-13 mixtures with larger, more isolated voids. This finding challenges the conventional belief that air void content correlated to oxygen diffusion rate, highlighting the need for refinement in existing Multiphysics oxidative aging models.
(2) Field monitoring demonstrated complex interactions between environmental factors and oxygen transport behaviors in asphalt

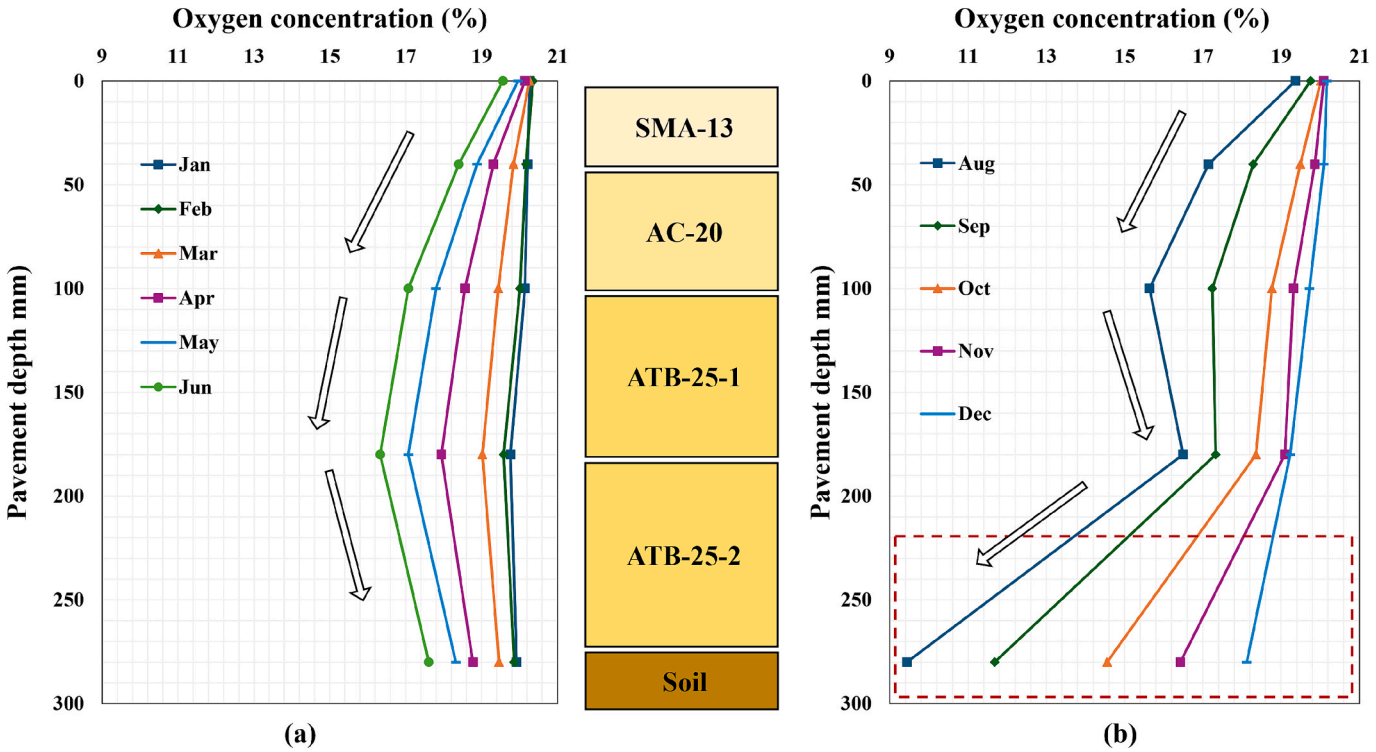

Fig. 16. The depth profile of oxygen concentration in the trial section.

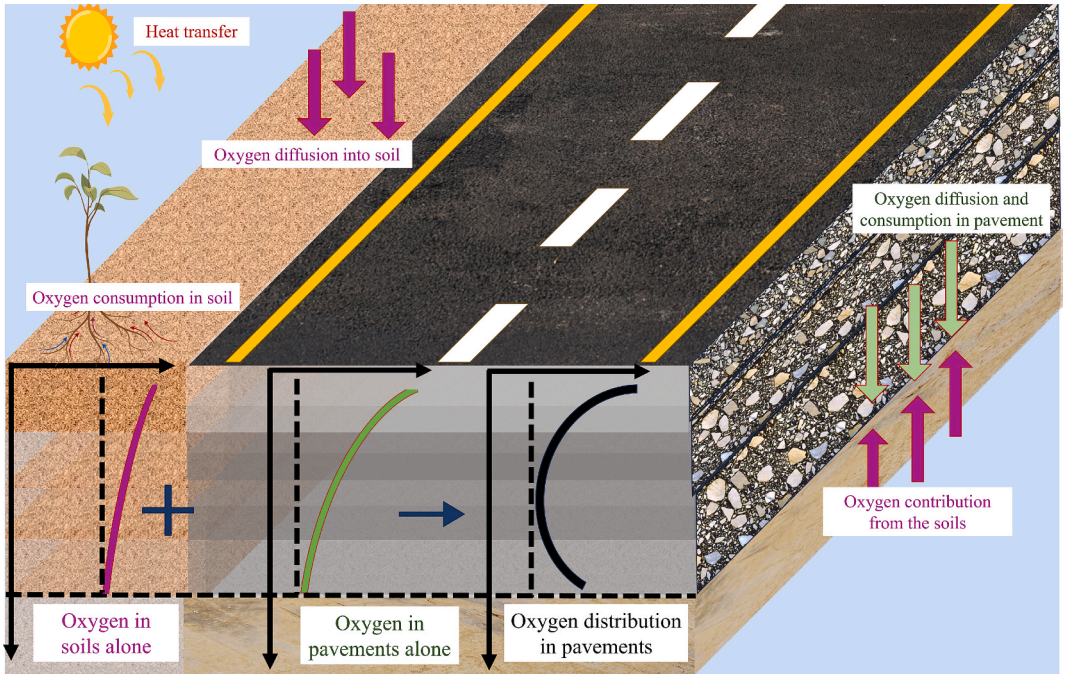

Fig. 17. A bidirectional oxygen diffusion model.

pavements. Temperature profiles showed clear seasonal variations, with attenuation of temperature fluctuations at greater depths. Moisture monitoring indicated that water infiltration during heavy rainfall events can persist within pavement layers, potentially threatening the performance of asphalt pavements.

(3) Most notably, the field oxygen concentration data revealed a non-monotonic, arc-shaped distribution with depth, contradicting the traditional assumption of unidirectional attenuation of aging. The observed patterns were explained by a bidirectional oxygen diffusion model, wherein oxygen is supplied both from the atmosphere above and the soil below, with the latter acting as a secondary source under certain conditions.

These findings underscore the importance of considering both mixture design, pavement structure, and environmental interactions in predicting and mitigating oxidative aging in asphalt pavements. The results also demonstrate the limitations of current aging models, particularly the treatment of oxygen transport and boundary conditions. Based on these findings, several recommendations are proposed for future research and applications in the field of asphalt pavement aging:

(1) Current Multiphysics oxidative aging models should be refined to account for the influence of air void connectivity and the realistic boundary conditions of oxygen.
(2) The bidirectional diffusion model of oxygen between pavement and underlying soil layers needs further investigation. Future studies should focus on quantifying the contribution of soil as an oxygen source or sink, and on understanding the impact of soil moisture and biological activity on oxygen dynamics.
(3) Continued development and deployment of robust, high-precision sensors for in-situ monitoring of oxygen, temperature, and moisture are recommended. Improved sensor durability and data acquisition systems will enhance the reliability of long-term field studies.
(4) Long-term, high-resolution field monitoring of oxygen, temperature, and moisture should be expanded to different climatic regions and pavement structures. This will provide a broader dataset for validating and calibrating pavement aging predictive models and improving pavement durability.

CRediT authorship contribution statement

Xingyu Chen: Writing – review & editing, Writing – original draft, Methodology, Investigation, Formal analysis, Data curation, Conceptualization. **Yuhong Wang:** Writing – review & editing, Supervision, Methodology, Funding acquisition, Conceptualization. **Yinghao Miao:** Writing – review & editing, Resources, Methodology, Data curation. **Xingyi Zhu:** Writing – review & editing, Resources, Methodology. **Haopeng Wang:** Writing – review & editing, Resources, Methodology. **Huailei Cheng:** Writing – review & editing, Investigation, Data curation.

Declaration of competing interest

The authors declare that they have no known competing financial interests or personal relationships that could have appeared to influence the work reported in this paper.

Acknowledgments

This paper is based on the research project (Project No. PolyU 15210321, 15202523) funded by the Research Grant Council of Hong Kong Special Administrative Region Government.

Data availability

All data generated or used during the study appears in the submitted article.

References

[1] X. Chang, R. Zhang, Y. Xiao, X. Chen, X. Zhang, G. Liu, Mapping of publications on asphalt pavement and bitumen materials: a bibliometric review, Constr. Build. Mater. 234 (2020) 117370.
[2] D. Jin, L. Yin, S. Nedrich, K.A. Boateng, Z. You, Resurface of rubber modified asphalt mixture with stress absorbing membrane interlayer: from laboratory to field application, Constr. Build. Mater. 441 (2024) 137452.
[3] A. Kargari, M. Arabani, S.M. Mirabdolazimi, Effect of palm oil capsules on the self-healing properties of aged and unaged asphalt mixtures gained by resting period and microwave heating, Constr. Build. Mater. 316 (2022) 125901.

[4] D. Jin, K. Xin, L. Yin, S. Mohammadi, B. Cetin, Z. You, Performance of rubber modified asphalt mixture with tire-derived aggregate subgrade, Constr. Build. Mater. 449 (2024) 138261.
[5] S.A. Saed, H. Ziari, N. Kamboozia, E.A. Dehaghi, Rheological and aging performance of reclaimed asphalt binders modified by warm mix additive and recycling agent, Sci. Rep. 15 (1) (2025) 44697.
[6] A. Jahandideh, S.M. Mirabdolazimi, M. Arabani, Effect of aging levels and induction factors on self-healing ability by induction heating method in hot asphalt mixtures, Case Stud. Constr. Mater. (2025) e05564.
[7] X. Zhu, R. Li, L. Jia, G. Hao, X. Chen, Y. Wang, Long-term property evolution of SBS-modified asphalt binders in simulated natural aging, J. Mater. Civ. Eng. 37 (8) (2025) 04025244.
[8] X. Chen, Y. Wang, H. Cheng, J. Wang, X. Zhu, Effects of accelerated aging conditions on the assessment of antioxidant effectiveness of asphalt binders, Constr. Build. Mater. 492 (2025) 143043.
[9] R. Zhang, N. Tang, H. Zhu, Y. Xi, R. Li, G. Hao, Long-term escape behavior and release mechanism of organic emissions from asphalt materials, Sci. Total Environ. 947 (2024) 174601.
[10] X. Chen, Y. Wang, Y. Wen, H. Cheng, G. Hao, J. Wang, Quantitative analysis of oxidative aging effects on the fatigue resistance of asphalt mixtures based on the simplified viscoelastic continuum damage (S-VECD) model, Int. J. Fatigue 177 (2023) 107916.
[11] J.C. Petersen, P.M. Harnsberger, Asphalt aging: dual oxidation mechanism and its interrelationships with asphalt composition and oxidative age hardening, Transp. Res. Rec. 1638 (1) (1998) 47–55.
[12] J.S. Chen, L.S. Huang, Developing an aging model to evaluate engineering properties of asphalt paving binders, Mater. Struct. 33 (9) (2000) 559–565.
[13] R. Davison, A.E. Martin, A. Chowdhury, R. Han, N. Prapaitrakul, X. Jin, J. Lawrence, Evaluation of binder aging and its influence in aging of hot mix asphalt concrete: literature review and experimental design, 2009.
[14] X. Jin, R. Han, Y. Cui, C.J. Glover, Fast-rate–constant-rate oxidation kinetics model for asphalt binders, Ind. Eng. Chem. Res. 50 (23) (2011) 13373–13379.
[15] N. Prapaitrakul, R. Han, X. Jin, C.J. Glover, A transport model of asphalt binder oxidation in pavements, Road Mater. Pavement Des. 10 (sup1) (2009) 95–113.
[16] Y. Wen, Y. Wang, Determination of oxygen diffusion coefficients of compacted asphalt mixtures, Constr. Build. Mater. 160 (2018) 385–398.
[17] X. Chen, Y. Wang, Y. Wen, H. Cheng, G. Hao, Oxygen diffusion coefficients of asphalt mixtures and their impacts on mixture aging, Transp. Res. Rec. (2023) 03611981221143117.
[18] X. Chen, Y. Wang, Conserving existing road pavements against aging: a new assessment method and evaluation of different techniques, J. Clean. Prod. 446 (2024) 141498.
[19] N. Prapaitrakul, R. Han, X. Jin, C.J. Glover, A transport model of asphalt binder oxidation in pavements, Rd Materials & Pavement Design. 10/SI (2009) 95–113.
[20] R. Han, Improvement to a transport model of asphalt binder oxidation in pavements: pavement temperature modeling, oxygen diffusivity in asphalt binders and mastics, & pavement air void characterization, Texas A&M Univ, 2011. Ph.D. dissertation.
[21] Y. Zheng, Y. Cai, Y. Zhang, Study on temperature field of asphalt concrete pavement, In Emerging Technologies for Material, Design, Rehabilitation, and Inspection of Roadway Pavements, 2011, (pp. 266-273).
[22] Y. Li, L. Liu, L. Sun, Temperature predictions for asphalt pavement with thick asphalt layer, Constr. Build. Mater. 160 (2018) 802–809.
[23] D.M. Mrawira, J. Luca, Thermal properties and transient temperature response of full-depth asphalt pavements, Transp. Res. Rec. 1809 (1) (2002) 160–171.
[24] M.W. Mirza, Development of a global aging system for short and long term aging of asphalt cements, University of Maryland, College Park, 1993.
[25] F. Yin, A.E. Martin, E. Arámbula-Mercado, D. Newcomb, Characterization of non-uniform field aging in asphalt pavements, Constr. Build. Mater. 153 (2017) 607–615.
[26] X. Luo, F. Gu, R.L. Lytton, Prediction of field aging gradient in asphalt pavements, Transp. Res. Rec. 2507 (1) (2015) 19–28.
[27] M.D. Elwardany, F.Y. Rad, C.A.S.S.I.E. Castorena, Y.R. Kim, Climate-, depth-, and time-based laboratory aging procedure for asphalt mixtures, J. Assoc. Asphalt Paving Technol. 87 (2018) 467–511.
[28] P. Singhvi, J.J.G. Mainieri, H. Ozer, B.K. Sharma, I.L. Al-Qadi, K.L. Morse, Impacts of field and laboratory long-term aging on asphalt binders, Transp. Res. Rec. 2676 (8) (2022) 336–353.
[29] P.Y. Wang, Y. Wen, K. Zhao, D. Chong, A.S. Wong, Evolution and locational variation of asphalt binder aging in long-life hot-mix asphalt pavements, Constr. Build. Mater. 68 (2014) 172–182.
[30] MnDOT, 2012. MnROAD data release user's guide, www.mndot.gov/mnroad.
[31] Y. Wang, K. Zhao, F. Li, Aging–Depth Relationship of Asphalt Binders in Hot-Mix Asphalt Pavements (No. 18-05687), 2018.
[32] Long-Term Pavement Performance (LTPP), 2025. Available from: https://infopave.fhwa.dot.gov/.
[33] E.L. Omairey, F. Gu, Y. Zhang, An equation-based multiphysics modelling framework for oxidative ageing of asphalt pavements, J. Clean. Prod. 280 (2021) 124401.
[34] E.L. Omairey, Y. Zhang, H. Soenen, X. Carbonneau, Parametric analysis and field validations of oxidative ageing in asphalt pavements using multiphysics modelling approaches, Int. J. Pavement Eng. 24 (2) (2023) 2020267.
[35] K.M. Lunsford, The effect of temperature and pressure on laboratory oxidized asphalt films with comparison to field aging (Doctoral dissertation), 1994.
[36] C.J. Glover, R. Han, X. Jin, N. Prapaitrakul, Y. Cui, A. Rose, J.J. Lawrence, M. Padigala, E. Arambula, E.S. Park, A.E. Martin, Evaluation of binder aging and its influence in aging of hot mix asphalt concrete: Technical report (No. FHWA/TX-14/0-6009-2), 2014.
[37] R. Han, X. Jin, C.J. Glover, Modeling pavement temperature for use in binder oxidation models and pavement performance prediction, J. Mater. Civ. Eng. 23 (4) (2011) 351–359.
[38] F. Han, X. Zhang, J. Yu, S. Xu, G. Zhou, S. Li, Study on spatiotemporal dynamic characteristics of precipitation and causes of waterlogging based on a data-driven framework, Sci. Total Environ. 913 (2024) 169796.
[39] H.L. Penman, Gas and vapour movements in the soil: I. the diffusion of vapours through porous solids, J. Agric. Sci. 30 (3) (1940) 437–462.
[40] A. Sallam, W.A. Jury, J. Letey, Measurement of gas diffusion coefficient under relatively low air-filled porosity, Soil Sci. Soc. Am. J. 48 (1) (1984) 3–6.